

## CASE STUDY OF A DESICCANT EVAPORATIVE COOLING SYSTEM IN A DANISH OFFICE BUILDING: SYSTEM MODELING FROM LONG-TERM MONITORING DATA

Alanis Zeoli<sup>1\*</sup>, Samuel Gendebien<sup>1</sup>, Hicham Johra<sup>2</sup>, Vincent Lemort<sup>1</sup>

<sup>1</sup>Liège University, Applied Thermodynamics Laboratory, Department of Aerospace and Mechanics, Liège, Belgium

<sup>2</sup>Aalborg University, Department of the Built Environment, Aalborg, Denmark

\*Corresponding Author: alanis.zeoli@uliege.be

### ABSTRACT

With global warming, the demand for cooling energy is expected to increase, even in moderate-climate regions. In heating-dominated countries equipped with a district heating network (DHN), the usage of the DHN in summer is reduced and low-grade energy in the form of heat is widely available. Denmark has implemented a pilot project to harness low-grade energy from its local DHN to provide cooling to buildings using evaporative cooling technologies. The pilot project building is an office building equipped with a desiccant evaporative cooling system (DECS). The latter has been monitored to allow a direct and accurate assessment of the energy performance of such HVAC systems. In the present paper, a model of the DECS installation has been developed. Based on long-term monitoring, the ability of the model to predict the behaviour of the system components and to simulate the system control strategy has been studied. Despite the limitations due to the monitoring setup and the simplifying assumptions of the numerical model, it was established that the model fairly predicts real DECS behaviour, regarding supply air conditions, energy and water consumption and system operation.

### 1 INTRODUCTION

In recent decades, the demand for cooling buildings has steadily increased, and with the ongoing effects of global warming, this trend can only intensify. Cooling accounts for nearly 20% of the total electricity demand of buildings worldwide (Biol, 2018). Alternative air-conditioning methods have become a significant area of interest to tackle the drawbacks of vapour-compression systems, such as their high-grade energy need and reliance on refrigerants with sustainability issues. Desiccant evaporative cooling technologies offer a promising solution, primarily utilising low-grade energy sources like solar energy or waste heat from industrial processes. Additionally, these technologies can leverage district heating networks (DHN) during the summer months when there is less demand for heating.

In the authors' previous work (Zeoli et al., 2023), the integration of a desiccant cooling system with evaporative cooling technologies has been widely studied. The study demonstrated that desiccant evaporative cooling systems (DECS) can be used in most climates, with optimal efficiency observed in dry climate conditions. This current study aims to delve deeper into the feasibility of DECS, with a focus on system operation. A Danish pilot project has been developed to promote the use of the DHN in summer as a heat source for space cooling via evaporative cooling technology, thus reducing the stress on the electric network and tackling the decarbonisation of cooling (Pacak & Chorowski, 2023).

### 2 METHODOLOGY

A DECS has been installed in a five-floor office building with a ground surface of 5000 m<sup>2</sup> in Denmark. The DECS has a nominal air flow rate of 15 000 m<sup>3</sup>/h and can cover the cooling demand of one zone (out of six) of the building, demonstrating improved thermal comfort in the building compared to areas without mechanical cooling. The system is equipped with a complete monitoring system, detailed in

section 2.2. The results of the monitoring are used to calibrate the models of the main components of the system. Based on the thorough study of the system, some variants of the control strategy can be proposed to decrease the energy consumption associated with cooling. A detailed description of the evaporative cooling system and the building study case can be found in a dedicated technical report (Johra, 2021). The measurement data during the monitoring period of Spring and Summer 2022 can be downloaded from an open-access repository (Johra, 2024).

### 2.1 System description

A schematic representation of the DECS is presented in Figure 1a. The DECS serves both as a mechanical ventilation system and a cooling system. Fresh air from the outdoor environment is brought into the DECS and is then supplied to the conditioned space at a nearly constant temperature range of 16-18°C. The system consists of five main components. Initially, the hot and humid outdoor air (referred to as “process air”) is dehumidified and heated in a desiccant wheel (DW). Subsequently, it undergoes sensible cooling in a heat recovery wheel (HEX) before being humidified in a direct evaporative cooler (DEC 1). Additional heating or cooling (depending on the season) can be provided through an additional heat exchanger. The secondary air of the system, extracted from the conditioned space, is referred to as “regeneration air” since it is used to regenerate the DW by absorbing excess moisture removed from the process air. The exhaust air can be humidified in a direct evaporative cooler (DEC 2) before entering the HEX as secondary air. The regeneration air temperature is then increased to the DW regeneration temperature through a heat exchanger called the “regenerator” which is supplied with hot water from the DHN. Finally, the air enters the DW for regeneration.

The evolution of the process and regeneration air conditions are illustrated on a psychrometric chart in Figure 1b. The fresh air, initially at 32°C and 34% relative humidity (RH) is supplied to the building at 19.4°C and 78%. The system effectively maintains acceptable thermal comfort conditions, with indoor conditions of 24.6°C and a relative humidity of 56%, even during warm periods.

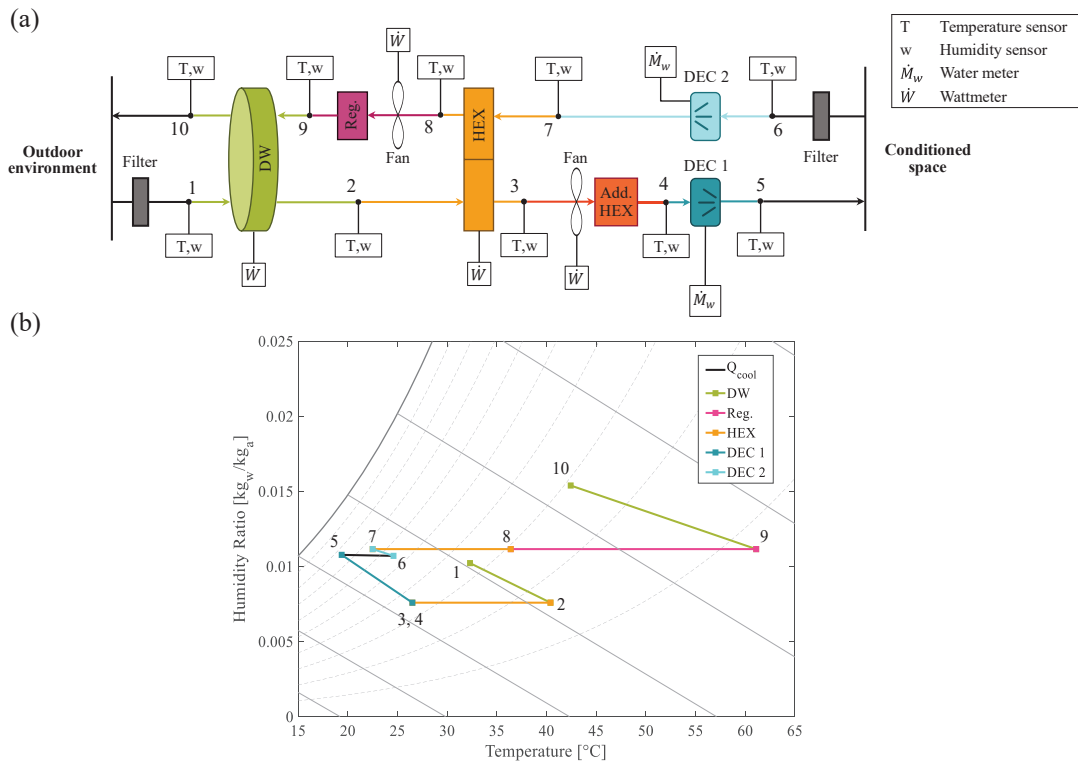


**Figure 1** (a) Schematic representation of the studied DECS with sensor instrumentation. (b) Evolution in the psychrometric diagram for outdoor conditions of 32°C and 34% RH.

## 2.2 Monitoring

The monitoring of the system is illustrated in Figure 1a and involves temperature and humidity, air flow rate, electricity, and water consumption measurements. Data is recorded every 30 seconds. The monitoring solutions are described below.

Temperature and humidity measurement. Temperature and humidity transducers are placed in between all components. The characteristics of the sensors are given in Table 1.

**Table 1:** P18S temperature and humidity transducer characteristics.

	Measuring range	Error
Temperature	-20 – 60°C	±0.6 K in range 10 – 40°C ±1 K in remaining range
Relative humidity	0 – 100%	±3% in range 10 – 90% ±5% in remaining range

Electricity and water consumption. The electricity consumption of the components (fan, DW motor, and HEX motor) is monitored through wattmeters while the water consumption is deduced from a water meter. The two water meters are placed before the two direct evaporative coolers.

Air flow rate measurement. The system is not equipped with a direct air flow rate measurement device. The air flow rate in the installation is deduced from the fan performance curves based on the electricity consumption of the fan and the head loss measurement across the fan. Since the flow rate computation is impacted by the measurement of the electricity consumption and the pressure losses, the relative error on the result has been assumed to be 5%.

## 2.3 Model of components

The components of the system have been modelled in MATLAB using simplified models that have been calibrated based on the monitoring data.

Rotating heat exchanger. The heat exchanger has been modelled with the  $\varepsilon$ -NTU model. The average heat transfer coefficient (AU) of the HEX has been determined using data from the monitoring campaign. It has been assumed that the AU coefficient varies with the air flow rate following an exponential relationship (Lebrun et al., 2004), as shown in Equation (1).

$$AU = AU_{nom} \cdot \left( \frac{\dot{M}_a}{\dot{M}_{a,nom}} \right)^m \quad (1)$$

It has been observed that the HEX can have a start and stop behaviour when the temperature at the inlet of the primary side is close to the minimum supply temperature. Given that the indoor temperature is above the maximum supply temperature, the latter can be exceeded, resulting in an ON/OFF control of the HEX. Subsequently, the heat transfer coefficient of the HEX should also account for part load operation. An exponential law has been assumed to be the most suitable model for that purpose. The system thermal inertia during ON/OFF operation is considered using the part load ratio (PLR) of the HEX. The NTU of the heat exchanger can thus be determined using Equation (2). An indicator of the PLR is the ratio of average to nominal power consumption of the HEX, as shown in Equation (3).

$$NTU = NTU_{nom} \cdot \left( \frac{\dot{M}_a}{\dot{M}_{a,nom}} \right)^{m-1} \cdot PLR^n \quad (2)$$

$$PLR = \frac{W_{HEX}}{W_{HEX,nom}} \quad (3)$$

The determination of the  $n$  coefficient is detailed in Section 3.1.

Desiccant wheel. The DW is a rotating heat exchanger. As shown in Figure 2, the inner matrix is made of aluminium foils wrapped around each other and covered by silica gel, a desiccant material. As primary air passes through the DW, moisture is absorbed by the desiccant material and stored in liquid

form. During the liquefaction process, heat is released and absorbed by the primary air flow which leaves the DW heated and dehumidified. On the secondary side, the regeneration process occurs by transferring heat to the desiccant material to evaporate water into the air stream. The DW model is based on a simplified empirical model developed by Panaras et al. (2010) and described in Equations (4) and (5). It relies on two main parameters  $\eta_{F1}$  and  $\eta_{F2}$  which can be calibrated using the monitoring data when the DW is activated. In the equations below,  $i = 1, 2, 9$  (cf. Figure 1) and  $j = 1, 2$ .

$$F_{1,i} = \frac{-2865}{(T_i + 273.15)^{1.49}} + 4.344 \cdot w_i^{0.8624} \quad \text{and} \quad F_{2,i} = \frac{(T_i + 273.15)^{1.49}}{6360} - 1.127 \cdot w_i^{0.07969} \quad (4)$$

$$\eta_{Fj} = \frac{F_{j,2} - F_{j,1}}{F_{j,9} - F_{j,1}} \quad (5)$$

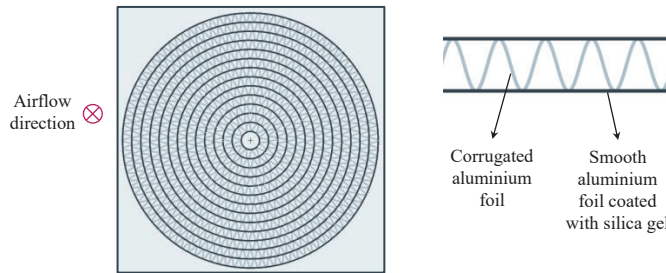


Figure 2: Simplified schematic of the desiccant wheel.

**Direct evaporative cooler.** The system comprises two DEC modules. DEC 2 is used to cool the air on the regeneration side, which is subsequently used as the secondary fluid in the HEX for pre-cooling the process air. DEC 1 is used to achieve the target supply temperature by further cooling the process air. The two modules have different operation modes. A simplified schematic of the DEC on the process side is given in Figure 3. The DEC consists of a porous material matrix that absorbs water. As air passes through this matrix, water evaporates, resulting in a cooling effect. The DEC is divided into three sections, each with a dedicated feeding pipe. Control stage valves on each pipe enable partial DEC operation. Water is temporarily stored in the upper distribution reservoirs (DR), to ensure even water distribution within one stage of the DEC. Since the water meter is placed before the water distribution reservoirs, there can be a discrepancy between the water consumption monitored by the water meter and the actual evaporation rate inside the DEC at a given time. Unevaporated water is collected in the bottom reservoir before being drained to prevent water stagnation. The DEC has been modelled using the definition of the wet bulb efficiency given in Equation (6).

$$\epsilon_{wb} = f_{DEC} \cdot \frac{T_{su} - T_{ex}}{T_{su} - T_{wb,su}} \quad (6)$$

Where  $f_{DEC}$  is the fraction of DEC 1 that is covered by water. On the process side,  $f_{DEC}$  can take values between 0, 1/3, 2/3, and 1 depending on the number of activated stages. On the regeneration side, however, the DEC is made of only one section and there is no gradual operation of DEC 2.

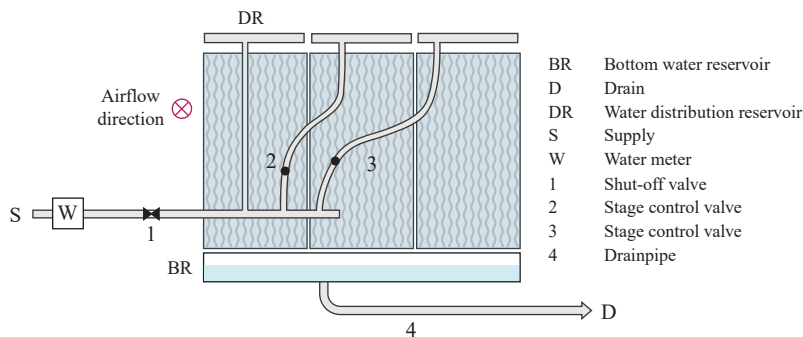
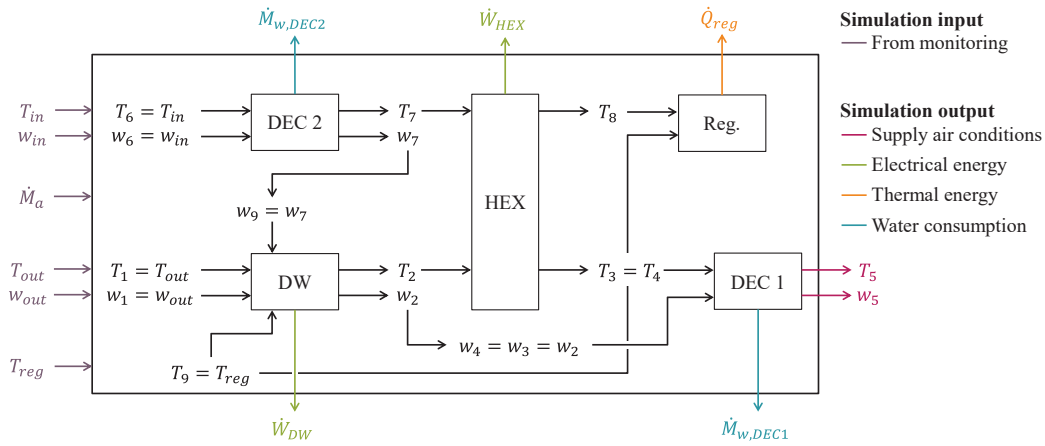


Figure 3: Simplified schematic of the direct evaporative cooler DEC 1.

**Fan.** The assessment of fan energy consumption is crucial for evaluating the energy performance of the installation. The air flow rate supplied to the building is considered an input of the model, enabling the evaluation of fan energy consumption. While it is commonly assumed that fan energy consumption is proportional to the cubed air flow rate (Bertagnolio, 2012), in this scenario, proportionality to the squared air flow rate has been identified as the most suitable one. The computation of fan energy consumption can therefore be carried out using Equation (7).

$$\dot{W}_{fan} = a \cdot \dot{M}_a^2 + b \cdot \dot{M}_a + c \quad (7)$$

The interaction between all the components for the resolution of the complete system is illustrated in Figure 4. The figure also shows the inputs and outputs of the model.



**Figure 4:** Resolution methodology implemented in MATLAB to compute the supply air conditions and the energy and water consumptions of the installation.

## 2.4 System operation

Depending on the outdoor conditions, the system can be operated in five different modes described below. The flow chart illustrating the process of determination of the current operation mode is presented in Figure 5. The control strategy of the system operation has been determined to ensure the target supply temperature while activating as few components as possible. The supply temperature should be between 16 and 18°C which are respectively referred to as  $T_{su,min}$  and  $T_{su,max}$ .

**Mode 1: Heat recovery.** When the outdoor temperature ( $T_{out}$ ) is below the minimum supply temperature ( $T_{su,min}$ ), the system operates in heat recovery mode. This mode activates the sensible heat exchanger and, if needed, the additional heat exchanger to ensure a supply air temperature close to the target supply temperature.

**Mode 2: Free chilling.** If the outdoor temperature is within the range of acceptable supply temperatures (16-18°C), the outdoor air can be directly supplied to the building by operating the system as a simple ventilation system.

**Mode 3: DEC.** If the outdoor temperature exceeds the maximum supply temperature ( $T_{su,max}$ ) but the wet bulb temperature ( $T_{wb,out}$ ) remains below the target supply temperature, it is possible to provide a cooling effect by activating the direct evaporative cooler on the process side (DEC 1).

**Mode 4: DECS.** If the outdoor specific humidity ( $w_{out}$ ) is higher than the nominal indoor specific humidity ( $w_{in,nom}$ ), the DW should be activated to dehumidify the supply air and prevent building humidification. The HEX and DEC 1 are activated to cool the air after passage into the DW. The nominal indoor conditions for thermal comfort have been set to 24°C and 50% (Morawska & Thai, 2018), which also corresponds to the average indoor conditions recorded during the monitoring period.

**Mode 5: DECS + DEC 2.** When DEC 1 fails to ensure an acceptable supply temperature, DEC 2 can be activated. This second DEC pre-cools the secondary air entering the sensible heat exchanger to lower the supply air temperature. However, the temperature of the regeneration air at the inlet of the regenerator is decreased, hence increasing the regeneration energy required by the system.

In the simulation, the deactivation of one component simply results in the bypass of this component in the resolution scheme described in Figure 4. At each time step, the operation mode of the system is determined based on the decision flow chart illustrated in Figure 5 and the operation mode is assumed constant during the whole time step. No partial operation of the DW and the HEX have been considered, except in heating mode where the HEX can operate with a PLR of 0.5.

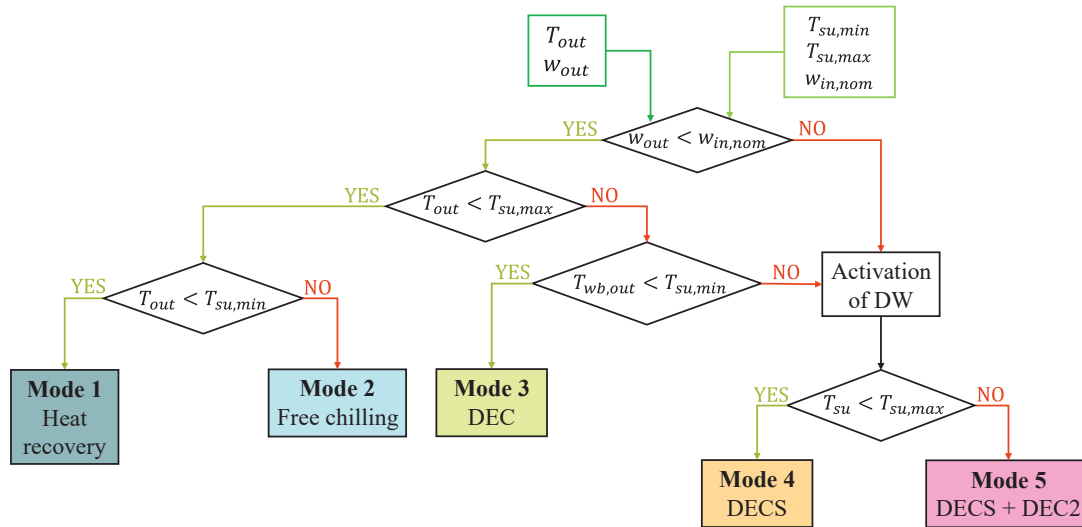


Figure 5: Decision flow chart for system operation.

### 3 RESULTS AND DISCUSSION

#### 3.1 Results of components sizing

**Rotating heat exchanger.** As introduced in section 2.2, an exponential model has been used to compute the NTU of the heat exchanger (Equation (2)). Two main factors impact the NTU: the ratio of actual to nominal air flow rates and the part load ratio of the HEX. When the flow rate is below the nominal value, the NTU of the heat exchanger is expected to increase, resulting in enhanced heat transfer. Lebrun et al. (2004) recommend a value of 0.8 for the value of the  $m$  factor.

As shown in Figure 6, three values of the  $n$  coefficients were tested to reproduce the behaviour of the HEX in ON/OFF mode. Firstly, it was assumed that partial operation of the HEX does not affect heat exchange ( $n = 0$ ). However, in heating mode, the exhaust temperature of the process air is overestimated. Secondly, it was assumed that the total heat transfer over time is directly proportional to the part load operation of the HEX ( $n = 1$ ). The exhaust temperatures are generally underestimated due to the thermal inertia of the heat exchanger matrix. Even though the HEX stops rotating, a heat transfer can persist due to brief start and stop cycles (approximately one minute). To account for inertia effects, it was found that the optimal value for the  $n$  coefficient is 0.7, which yields a 0.92 correlation coefficient between measured and simulated temperatures at HEX exhaust.

**Desiccant wheel.** The desiccant wheel factors  $\eta_{F1}$  and  $\eta_{F2}$  have been adjusted using the monitoring data. The calibration results are shown in Figure 7. The correlation coefficients between the measured and simulated conditions of the process air at the desiccant wheel outlet are 0.96 for temperature and 0.80 for specific humidity.

As introduced in Section 2.3, the DW model inputs are the temperature and humidity conditions at the DW inlet on the process side ( $T_1$  and  $w_1$ ) on the regeneration side ( $T_9$  and  $w_9$ ).  $T_1$  and  $w_1$  are the outdoor air conditions and are fixed to the measured values. As shown in Figure 4,  $w_9$  can be computed based on indoor conditions only. The monitored regeneration temperature  $T_9$  has also been considered a model input since there is no direct measurement of the regeneration energy consumption. Additionally, due to inertia effects, it takes time to reach the desired regeneration temperature. Establishing a simple rule to determine the regeneration temperature is challenging and it was therefore treated as an input parameter of the model.

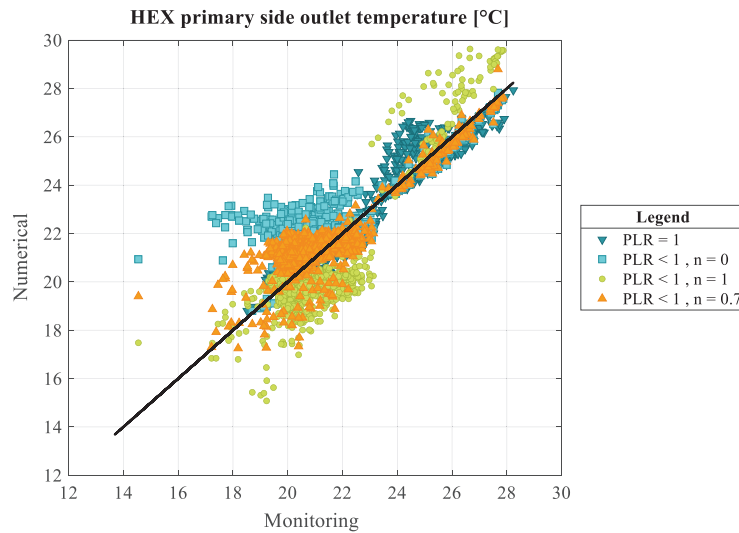


**Figure 6:** Measured and simulated values of the temperature at the heat exchanger exhaust on process side depending on the used law to describe HEX behaviour at part load.

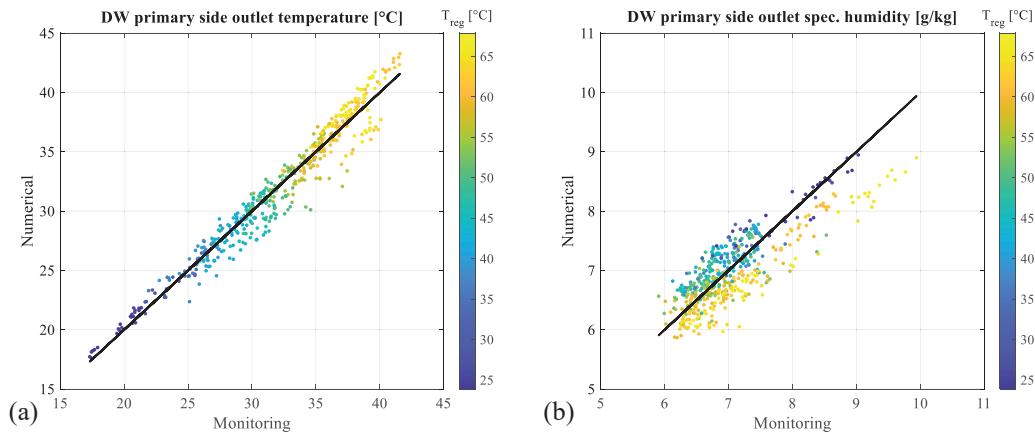


**Figure 7** (a) Measured and simulated process air temperature at DW outlet.  
 (b) Measured and simulated process air specific humidity at DW outlet.

Table 2 contains a summary of the parameters used in the components models.

**Table 2:** Summary of the model parameters.

DW		HEX		DEC		Fan	
$\eta_{F1}$	0.08	$NTU_{nom}$	3.98	$\varepsilon_{wb,max}$	0.85	$a$	292.7
$\eta_{F2}$	0.51	$m$	0.8	$f_{DEC,pro}$	{0, 1/3, 2/3, 1}	$b$	-422.6
$\dot{W}_{DW,nom}$	50 W	$n$	0.7	$f_{DEC,reg}$	{0, 1}	$c$	784.4
		$\dot{W}_{HEX,nom}$	110 W			$\dot{W}_{fan,nom}$	12 kW

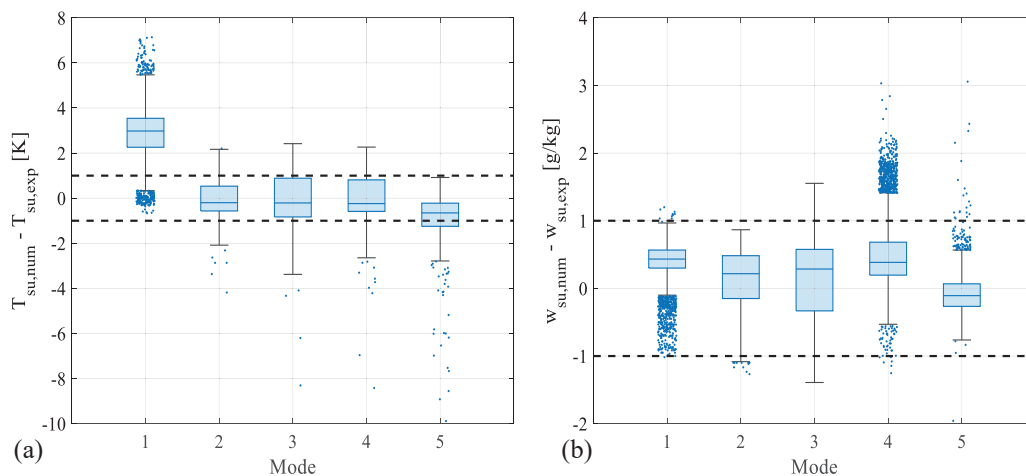
### 3.2 Comparison of the monitoring and simulation results

Figure 8 illustrates the difference between the simulated and measured building supply conditions. The temperature differences during the simulated period are gathered in a boxplot for each operation mode. The potential reasons for the difference between monitoring and simulation are discussed below.

In mode 1, *i.e.* heating mode, the numerical simulation tends to overestimate the supply temperature. As the outdoor temperature approaches the minimum supply temperature, the actual supply temperature can exceed the target supply temperature after the passage of the air through the HEX. In the actual system, an additional cooling coil (Add. HEX in Figure 1a) ensures the target temperature, but this component was not included in the model due to a lack of information on its performance, geometry, and controllability.

For the other modes, the predicted supply conditions are close to the measured conditions as the absolute temperature difference between simulated and monitored supply temperature mainly remains below 1 K. For most considered climatic conditions, the system effectively supplies the building with fresh air below 20°C. The negative temperature differences that can be observed mean that the simulation tends to underestimate the supply temperature, due to operational differences in the system mode. In the monitoring data, it appears that for those points the supply temperature is higher than 20°C and the system operates as a simple ventilation system in free chilling mode (mode 2), contrary to the predicted operation mode in the numerical model.

The discrepancies in supply specific humidity illustrated in Figure 8b for modes 1 and 2 can be attributed to humidity sensor measurement errors. In these modes, there is no (de)humidification of the outdoor air, the supply humidity should match the outdoor humidity, as imposed in the numerical model. However, comparisons with monitoring data show that supply humidity values are lower than outdoor specific humidity for modes 1 and 2, potentially due to sensor error. For the other modes, the supply specific humidity can be predicted with an accuracy of 1 g/kg.



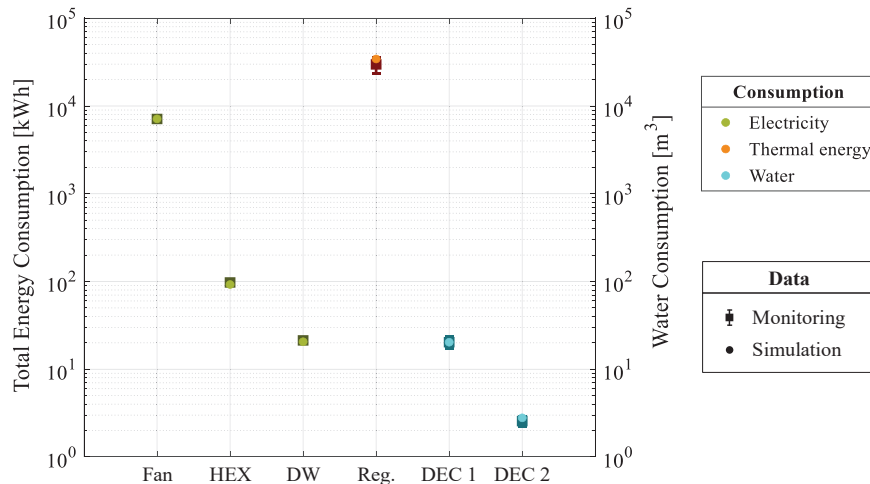
**Figure 8:** Difference between simulation and monitoring over the cooling period for each operation mode for (a) the supply temperature and (b) the supply specific humidity.

Figure 9 presents a comparison between monitoring data and simulation results regarding energy and water consumption. The consumption of all components was evaluated throughout the cooling season. For each consumption, an uncertainty analysis has been performed to determine how the uncertainty in each of the directly measured variables propagates into the value of the calculated quantity (Taylor & Kuyatt, 1994). The presented chart contains error bars, although for some consumptions they are too small to be visualised within the data markers.

The numerical model predicts total electricity consumption for fans and the rotating HEX with errors of 2.1% and 4.7%, respectively. During the cooling period, fan consumption totals 7 120 kWh, while HEX consumption amounts to 97 kWh. The energy consumption associated with the desiccant wheel rotation is well predicted with a small error rate of 3.3%, indicating the numerical model's capability to determine the need for wheel rotation. The electric energy consumption of the desiccant wheel amounts to 20 kWh over the cooling season, a negligible figure compared to the fan electricity consumption.

The regeneration energy accounts for the primary energy consumption of the system, utilizing four times more heat than electricity. However, this consumption is the most challenging to accurately estimate due to the lack of direct measurement. The regeneration energy consumption should be estimated based on air flow rate and temperature measurements upstream and downstream of the regenerator and can be significantly influenced by the precision of the sensors. The uncertainty on the calculated regeneration energy from the monitoring data has been estimated to be 18%.

In addition to electricity and heat, the DECS also consumes water. The total water consumption of DEC 1 amounts to 20.5 m<sup>3</sup> while the one of DEC 2 is only 2.8 m<sup>3</sup>, due to the rare operation in mode 5. Both consumptions are predicted within the uncertainty range of the monitored data.



**Figure 9:** Comparison of the total energy consumptions from the monitoring data and the results of the simulation.

Finally, it is also possible to study the ability of the model to predict the operation mode of the system. Figure 10 illustrates the system's real and predicted operation modes based on outdoor conditions on a psychrometric chart. Each point on the chart represents the outdoor conditions for one hour in the data set. The simple algorithm seems to effectively predict the system's operation mode.

Table 3 compares the number of hours in each mode for monitoring and simulation, revealing some noticeable differences that may have various explanations. There are two conflicting effects observed in predicting the system's operation in mode 1. When the outdoor specific humidity exceeds the indoor value but the temperature is below 15°C, the system operates in mode 1 instead of mode 4. For outdoor temperatures near the minimum supply temperature, the real system operates either in modes 1, 2, or 3.

This variability is due to mode 1 alone leading to supply temperatures above the maximum supply temperature, given the high efficiency of the HEX. The real control algorithm of the system might rely on the measurement of the supply temperature, which leads the system to operate in mode 2 and, subsequently, mode 3, due to system inertia. Mode 5 is the least accurately predicted, indicating the need for further investigation into the criteria for switching between modes 4 and 5.

From the above discussions, it can be concluded that the numerical model fairly predicts the behaviour of the installation, including the air conditions in the system, its energy consumption and its mode of operation.

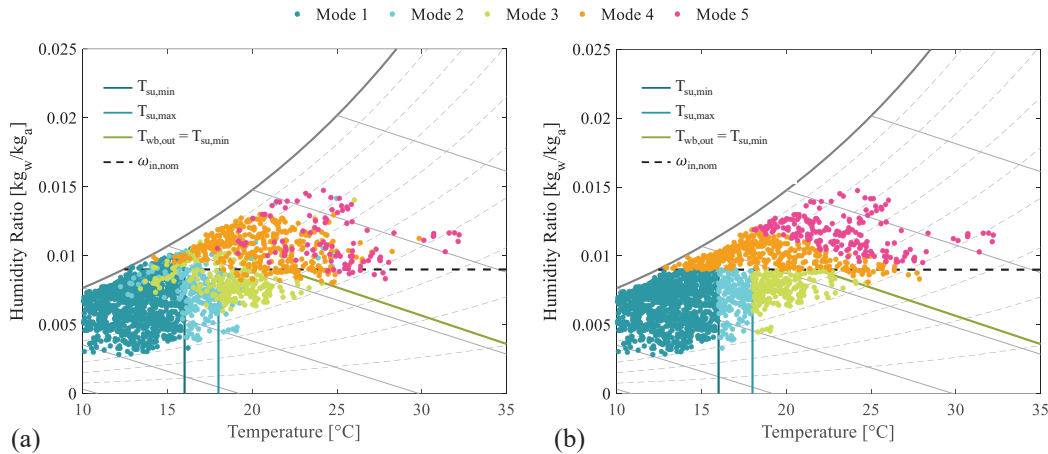


**Figure 10:** Operation mode of the system depending on the outdoor conditions according to (a) The real system operation, (b) The decision flow chart presented in Figure 5.

**Table 3:** Comparison of the number of hours of operation in each mode between the monitoring and the simulation.

	Mode 1	Mode 2	Mode 3	Mode 4	Mode 5
<b>Monitoring</b>	1560 h	253 h	280 h	362 h	105 h
<b>Simulation</b>	1520 h	190 h	243 h	412 h	195 h
<b>Difference</b>	-2.6%	-24.9%	-13.2%	+13.8%	+85.7%

### 3.3 Limitations

There can be discrepancies between monitoring and simulation results due to several factors, including limitations within the system or simplifications made in the numerical model.

#### Errors from the real system.

- Measurement errors: the sensitivity of sensors can lead to errors within a range of +/- 0.6 K for temperature and +/- 3% for RH measurements (cf. Table 1).
- Sensor placement: in a compact system, non-uniform air flow distribution can result in temperature and humidity measurements that differ from the average between components.
- System malfunctions: the system does not perform as expected, failing to achieve the target supply temperature despite simulations suggesting it is feasible under proper operation.

#### Errors from the simulation.

- Steady-state assumption: simplified models assume all components are in steady-state operation, while real-world transitions between modes may exhibit inertia effects.

- Simulation time step: the impact of time step size on results is significant, with smaller time steps capturing system dynamics more accurately but potentially causing dependency on previous steps, while larger time steps may overlook mode changes within the same step.
- System operation: the model assumes instantaneous system control based on current outdoor conditions, whereas real-world system operation may adapt based on past supply air conditions.

### 3.4 Propositions of improvement

Based on the findings of the previous sections, there are potential improvements that could enhance the energy efficiency of the system.

Optimizing heat transfer. In mode 1, where an additional cooling coil maintains the supply temperature around 18°C, energy consumption could be reduced by partially bypassing the HEX or adjusting the HEX rotational speed to vary the heat exchange coefficient based on heat demand. This optimization could save approximately 5 630 kWh of chilled water production, equivalent to around 2 200 kWh of electricity if the water is generated with a 2.5-COP chiller.

Introducing Indirect Evaporative Cooling (IEC). Replacing the sensible heat exchanger with an indirect evaporative cooling module presents another improvement opportunity. The IEC operates similarly to a direct evaporative cooling system but with the distinction that the air to be cooled down is not in direct contact with water. Instead, the cooling process occurs through heat transfer between wet and dry channels. The IEC can function in both wet and dry modes, eliminating the need for a DEC on the regeneration side and reducing head losses in the system. Additionally, the IEC is more efficient than a sensible HEX combined with a DEC as a pre-cooler on the secondary side. By potentially producing process air at a lower temperature, the reliance on further cooling in the DEC could be minimized, leading to decreased water consumption.

## CONCLUSION

This work contributes to evaluating the potential of evaporative cooling technologies. A desiccant evaporative cooling system (DECS) was installed in an office building in Denmark. The DECS is equipped with a complete monitoring system providing data for spring and summer 2022. The data was analysed in detail and used to calibrate simplified component models. The models were then used to simulate the system behaviour and evaluate the system consumption during the cooling period.

A simplified control strategy of the DECS was established based on the operating limits of the components. It was demonstrated that the DECS model effectively predicts the supply air conditions for the considered outdoor climatic conditions with an accuracy of 1 K and 1 g/kg. The DECS is characterised by electricity, heat and water consumption. The electricity consumption associated with the rotation speed of the fan, the HEX and the DW as well as the water consumption of the direct evaporative coolers can be predicted with an accuracy of 95%. The difference between the monitored and simulated thermal energy consumption of the regenerator remains in the uncertainty range associated with measurement errors. It was also shown that the simplified control strategy implemented in the numerical model allows to fairly predict the operation mode of the system to provide adequate supply air conditions. Finally, two ideas for improvement were proposed to decrease the system energy consumption.

## NOMENCLATURE

Abbreviations		Symbols	
DEC	Direct evaporative cooler/cooling	$a, b, c$	Fan parameters [-]
DECS	Desiccant evaporative cooling system	$\varepsilon_{wb}$	Wet bulb efficiency [-]
DHN	District heating network	$f_{DEC}$	Fraction of DEC covered by water [-]
DW	Desiccant wheel	$\dot{M}$	Mass flow rate [kg/s]
HEX	Heat exchanger	$m, n$	HEX parameter [-]
IEC	Indirect evaporative cooler/cooling	$\eta_{F1}, \eta_{F2}$	Desiccant wheel parameter [-]
PLR	Part load ratio	$T$	Temperature [°C]
Reg.	Regenerator	$T_{wb}$	Wet bulb temperature [°C]
RH	Relative humidity	$w$	Specific humidity [kg/kg]
		$\dot{W}$	Power consumption [W]
Subscripts			
a	Air	in	Indoor environment
w	Water	out	Outdoor environment
su	Supply air		

## REFERENCES

- Bertagnolio, S. (2012). *Efficient-based model calibration for efficient building energy services*. Université de Liège.
- Birol, D. F. (2018). The Future of Cooling—Opportunities for energy efficient air conditioning. *International Energy Agency*.
- Johra, H. (2021). *Instant District Cooling System: Project Study Case Presentation* (DCE Technical Reports 290). Department of the Built Environment, Aalborg University. <https://doi.org/10.54337/aau468741799>
- Johra, H. (2024). *Operation data of a desiccant evaporative cooling system implemented in an office building in Denmark during spring and summer 2022*. Zenodo.
- Lebrun, J., Silva, C. A., Trebilcock, F., & Winandy, E. (2004). Simplified models for direct and indirect contact cooling towers and evaporative condensers. *Building Services Engineering Research and Technology*, 25(1), 25–31. <https://doi.org/10.1191/0143624404bt088oa>
- Morawska, L., & Thai, P. (2018). Estimation of minimal risk and acceptable temperatures for selected cities. In *WHO Housing and health guidelines* (WHO/CED/PHE).
- Pacak, A., & Chorowski, M. (2023). *Challenges of air conditioning decarbonization*. [dataset]. Proceedings of 26th International Congress of Refrigeration, Paris. <https://doi.org/10.18462/IIR.ICR.2023.0666>
- Panaras, G., Mathioulakis, E., Belessiotis, V., & Kyriakis, N. (2010). Experimental validation of a simplified approach for a desiccant wheel model. *Energy and Buildings*, 42(10), 1719–1725. <https://doi.org/10.1016/j.enbuild.2010.05.006>
- Taylor, B. N., & Kuyatt, C. E. (1994). *NIST Technical note 1297*. Guidelines for evaluating and expressing the uncertainty of NIST measurement results.
- Zeoli, A., Gendebien, S., & Lemort, V. (2023). Performance evaluation of a desiccant cooling system coupled with indirect evaporative cooling technologies under various climates. *Refrigeration Science and Technology Proceedings*, 4, 270–280. <https://doi.org/10.18462/iir.icr.2023.0471>

## ACKNOWLEDGEMENT

This study is a part of the International Energy Agency (IEA) EBC Annex 85 – “Indirect Evaporative Cooling” project activities.